The Astrophysical Journal, 734:7 (10pp), 2011 June 10 doi:10.1088/0004-637X/734/1/7

THE SOLAR ORIGIN OF SMALL INTERPLANETARY TRANSIENTS

A. P. Rouillard[1,2], N. R. Sheeley, Jr.[3], T. J. Cooper[3], J. A. Davies[4], B. Lavraud[5,6], E. K. J. Kilpua[7], R. M. Skoug[8], J. T. Steinberg[8], A. Szabo[2], A. Opitz[5,6], and J.-A. Sauvaud[5,6]
[1] College of Science, George Mason University, Fairfax, VA 22030, USA
[2] NASA Goddard Space Flight Center, Greenbelt, Maryland, MD 20771, USA
[3] Naval Research Laboratory, Washington, DC 29375-5352, USA
[4] RAL Space, Rutherford Appleton Laboratory, Chilton, OX11 0QX, UK
[5] Centre d'Etude Spatiale des Rayonnements, Université de Toulouse, 21028, Toulouse, France
[6] Centre National de la Recherche Scientifique, UMR 5187, Toulouse, France
[7] Department of Physical Sciences, Theoretical Physics Division, University of Helsinki, Finland
[8] Space Science and Applications, Los Alamos National Laboratory, MS-D466, Los Alamos, NM 87545, USA
Received 2010 November 1; accepted 2011 February 21; published 2011 May 19

ABSTRACT

In this paper, we present evidence for magnetic transients with small radial extents ranging from 0.025 to 0.118 AU measured in situ by the *Solar-Terrestrial Relations Observatory* (*STEREO*) and the near-Earth *Advanced Composition Explorer* (*ACE*) and *Wind* spacecraft. The transients considered in this study are much smaller (<0.12 AU) than the typical sizes of magnetic clouds measured near 1 AU (∼0.23 AU). They are marked by low plasma beta values, generally lower magnetic field variance, short timescale magnetic field rotations, and are all entrained by high-speed streams by the time they reach 1 AU. We use this entrainment to trace the origin of these small interplanetary transients in coronagraph images. We demonstrate that these magnetic field structures originate as either small or large mass ejecta. The small mass ejecta often appear from the tip of helmet streamers as arch-like structures and other poorly defined white-light features (the so-called blobs). However, we have found a case of a small magnetic transient tracing back to a small and narrow mass ejection erupting from below helmet streamers. Surprisingly, one of the small magnetic structures traces back to a large mass ejection; in this case, we show that the central axis of the coronal mass ejection is along a different latitude and longitude to that of the in situ spacecraft. The small size of the transient is related to the in situ measurements being taken on the edges or periphery of a larger magnetic structure. In the last part of the paper, an ejection with an arch-like aspect is tracked continuously to 1 AU in the *STEREO* images. The associated in situ signature is not that of a magnetic field rotation but rather of a temporary reversal of the magnetic field direction. Due to its "open-field topology," we speculate that this structure is partly formed near helmet streamers due to reconnection between closed and open magnetic field lines. The implications of these observations for our understanding of the variability of the slow solar wind are discussed.

Key words: solar wind – Sun: corona – Sun: coronal mass ejections (CMEs) – Sun: heliosphere

1. INTRODUCTION

Interplanetary transients often contain highly organized magnetic fields that are detected in situ as continuous rotations of the magnetic field usually lasting between 12 hr and 2 days (Burlaga et al. 1981; Lepping et al. 2008). These rotations can be interpreted as the passage of a series of magnetic flux tubes that have been intertwined, probably during the formation and eruption of the transients, to form a "magnetic flux rope" (e.g., Gosling et al. 1995). Magnetic clouds are common examples of regions in the solar wind where the magnetic field direction changes smoothly and where, additionally, the magnetic field strength is high, the proton temperature and plasma beta are low compared to the ambient solar wind (Burlaga et al. 1981). The magnetic field pressure inside these magnetic flux ropes is often much higher than the plasma pressure. Therefore, the ropes appear in white-light images as dark "cavities" corresponding to regions where the electron density is low (Chen et al. 1997; Rouillard et al. 2009b). These cavities stand out from the darkness of the background sky because they are usually located between denser plasma structures which form the outline of large coronal mass ejecta (CMEs). White-light modeling, which assumes that most of the plasma observed in a CME is located on the surface of a "croissant-shaped" flux rope, has been used successfully to derive the three-dimensional topology and orientation of the underlying flux ropes (Thernisien et al. 2006; Rouillard et al. 2009b; Wood et al. 2010). Previous studies have shown that many CMEs retain their topology and orientation from the Sun to 1 AU (Marubashi 1986, 1991; Bothmer 2003). This is confirmed by the latest studies using data obtained by the *Solar-Terrestrial Relations Observatory* (*STEREO*) which show that the orientation of flux ropes inferred from white-light rendering techniques often match the orientation of magnetic flux ropes measured simultaneously in situ (Rouillard et al. 2009b; Wood et al. 2010; Möstl et al. 2009). This is a field of active research and more case studies are needed to confirm that the simple "croissant-shaped" flux-rope model is a valid description of CME topology.

The Lepping et al. (2008) list of magnetic cloud events measured in situ near 1 AU during the previous solar cycle shows that the duration of these events ranges from 5 to 43 hr with a mean duration of 22 hr. This broad range of values is related to the expansion rate of the magnetic cloud from the Sun to 1 AU (Klein & Burlaga 1982; Bothmer & Schwenn 1998; Démoulin & Dasso 2009); however, it is thought that other effects such as the different types and sizes of associated CMEs (Howard et al. 1985; St. Cyr et al. 2000) or the distance between the central axis of the flux rope and the point of in situ measurement (e.g., Farrugia et al. 2011) must also play a role. Out of the 53 magnetic clouds listed by Lepping et al. (2008), only two were slow events (<400 km s^{-1}) lasting less than 13 hr. Similarly the broader list given by Liu et al. (2005) of ∼90 interplanetary

CMEs (ICMEs) measured near 1 AU contains only six slow events (<400 km s^{-1}) with durations of less 13 hr. The origin and nature of magnetic field rotations lasting less than half a day but longer than the typical duration of Alfvén waves observed in the near-ecliptic solar wind (<3 hr; Belcher & Davis 1971; Smith et al. 1995) are very poorly understood. These transients represent the lower end of a large spectrum of interplanetary ejecta durations which are the subject of this paper.

The results of statistical analyses of small magnetic field rotations measured in situ are more than ambivalent; Cartwright & Moldwin (2008) suggest that small- and large-scale flux ropes originate by different source mechanisms, whereas Feng et al. (2008) conclude that all magnetic flux ropes detected in situ are the signatures of CMEs. However, the lists of small magnetic flux ropes presented by these authors differ, perhaps as a result of the different criteria used to identify these features. Rotations of the magnetic field vector measured during the passage of long duration Alfvén waves (Tsurutani et al. 1996) or even torsional Alfvén waves (Marubashi et al. 2010) could be easily mistaken for magnetic flux ropes without an associated analysis of the velocity component. The recent discovery of a torsional Alfvén wave embedded inside a magnetic flux rope measured in solar wind data taken near the L1 Lagrange point (Gosling et al. 2010) highlights the difficulties that can be encountered when distinguishing large-amplitude, long-duration Alfvén waves from magnetic flux ropes on timescales of less than 12 hr.

The study of small-scale transients is particularly pertinent in the light of the recent discovery, made using observations from the *Sun–Earth Connection Coronal and Heliospheric Investigation* (*SECCHI*) package (Howard et al. 2008) on board *STEREO*, that streamer blobs are the edge-on views of small arches or loops that appear to be continually ejected from the tips of helmet streamers (Sheeley et al. 2009). In the present paper, we investigate the solar origin of magnetic field rotations lasting less than half a day that were measured in situ by the *Advanced Composition Explorer* (*ACE*), *Wind,* and *STEREO* spacecraft during the year interval 2007–2009. Feng et al. (2008) point out that small flux ropes would not have detectable white-light signatures because they are often associated with very weak density enhancements. To successfully trace these small-scale transients back to the Sun, we only consider magnetic structures that have been swept up by high-speed streams (HSSs) during their transit to 1 AU. Indeed, Sheeley & Rouillard (2010) have recently shown that small mass ejecta, and in particular streamer arches, which would otherwise expand and disappear rapidly in white-light images can be tracked in white-light images from the Sun to at least 1 AU if they are caught up and compressed by HSSs from coronal holes.

The result of our analysis suggests that in situ measurements of small magnetic field rotations can occur when a spacecraft intersects a small section of a large magnetic flux rope or when it intersects an intrinsically small ejection. Some small ejecta are already apparent in *STEREO*/COR-1 and seem to erupt from the chromosphere; others only appear in the COR-2 field of view slightly above helmet streamers (>3–4 $R_{\odot}$). These small ejecta can appear like loops extending over a small range of position angles (<15°) or slightly more extensive arch-like structures.

2. IN SITU MEASUREMENTS OF SMALL TRANSIENTS:

Each of the *STEREO* spacecraft carries a comprehensive suite of in situ instrumentation measuring the properties of the solar wind ions (Galvin et al. 2008), the magnetic field (Luhmann et al. 2008), and suprathermal electrons (Sauvaud et al. 2008). Corresponding measurements are obtained by the *ACE* (MAG: Smith et al. 1998; McComas et al. 1998; Gloeckler et al. 1998) and *Wind* spacecraft (Ogilvie et al. 1995; Lepping et al. 1995; Lin et al. 1995), both located near the L1 Lagrange point. Six transient events with the properties listed above, selected from the *STEREO*, *ACE,* and *Wind* data during the 2007–2009 time interval, are shown in Figure 1. Due to the lack of continuous alpha particle and electron measurements for some of the L1 (*ACE* and *Wind*) and *STEREO* data, we assume alpha particle number density is 4% of the proton density, alpha particle temperatures of four times the proton temperature, and a constant electron temperature of 130,000 K. The latter assumption is consistent with the high-thermal conductivity of electrons and the low correlation of electron temperature with other solar wind parameters (e.g., Newbury et al. 1998 and references therein; Issautier et al. 2005). The total perpendicular pressure (P), also presented, is the sum of the magnetic pressure and the plasma thermal pressure perpendicular to the magnetic field. The discrepancy between our assumptions and the real values of alpha content and electron temperatures will slightly affect the plasma β and P profiles, but this procedure provides a more meaningful pressure profile than the ion pressure considered alone.

Our criteria for selecting a small transient are a rotation of the magnetic field lasting between ∼2 hr and ∼13 hr, reduced magnetic field fluctuations, and an associated drop in plasma β. This latter parameter is defined as the ratio of the plasma and magnetic field pressures. Periods when the plasma β parameter drops below 1 are often associated with the passage of magnetic flux ropes because they are usually associated with strong magnetic fields (Burlaga et al. 1981). For each event, we also required that the magnetic structure be compressed by HSSs to increase the ambient density and therefore our chances of determining their solar origin using white-light images. We did not require that the proton temperature be reduced inside the transient and therefore some are not magnetic clouds. The reduced temperature measured inside magnetic clouds and other types of interplanetary transients detected near 1 AU has been associated with the expansion of the transient between the Sun and 1 AU. The compressive effects of the HSSs on the transients considered in this study may have hampered their expansion and therefore prevented a temperature decrease inside the transients. We note that subparts of magnetic clouds can have high temperatures when they are located in compression regions (Burlaga et al. 2003; Rouillard et al. 2010a). When the components of the solar wind velocity are available (at L1 and *STEREO-A*), we also confirm that they are not correlated with the variations of the magnetic field components to exclude the possibility that these features are Alfvén waves.

To find transients with the signatures listed above, we visually inspected the in situ data measured by *STEREO* and at L1 during the 2007–2009 time interval and selected six events which fitted our criteria and are shown in Figure 1. They have differing radial extents, ranging from 0.025 to 0.118 AU (calculated by multiplying the duration of transient passage with the average radial speed of the transient), which are, as aforementioned, much smaller than the typical sizes of magnetic clouds (∼0.23 AU; Lepping et al. 2008). As we shall see, these six events appear to originate in a variety of sources near the Sun. Three of these events (2008 March 6, 2008 October 31, and 2008 August 15) appear in the list of interplanetary CMEs derived by Kilpua et al. (2009b). Table 1 presents some properties of

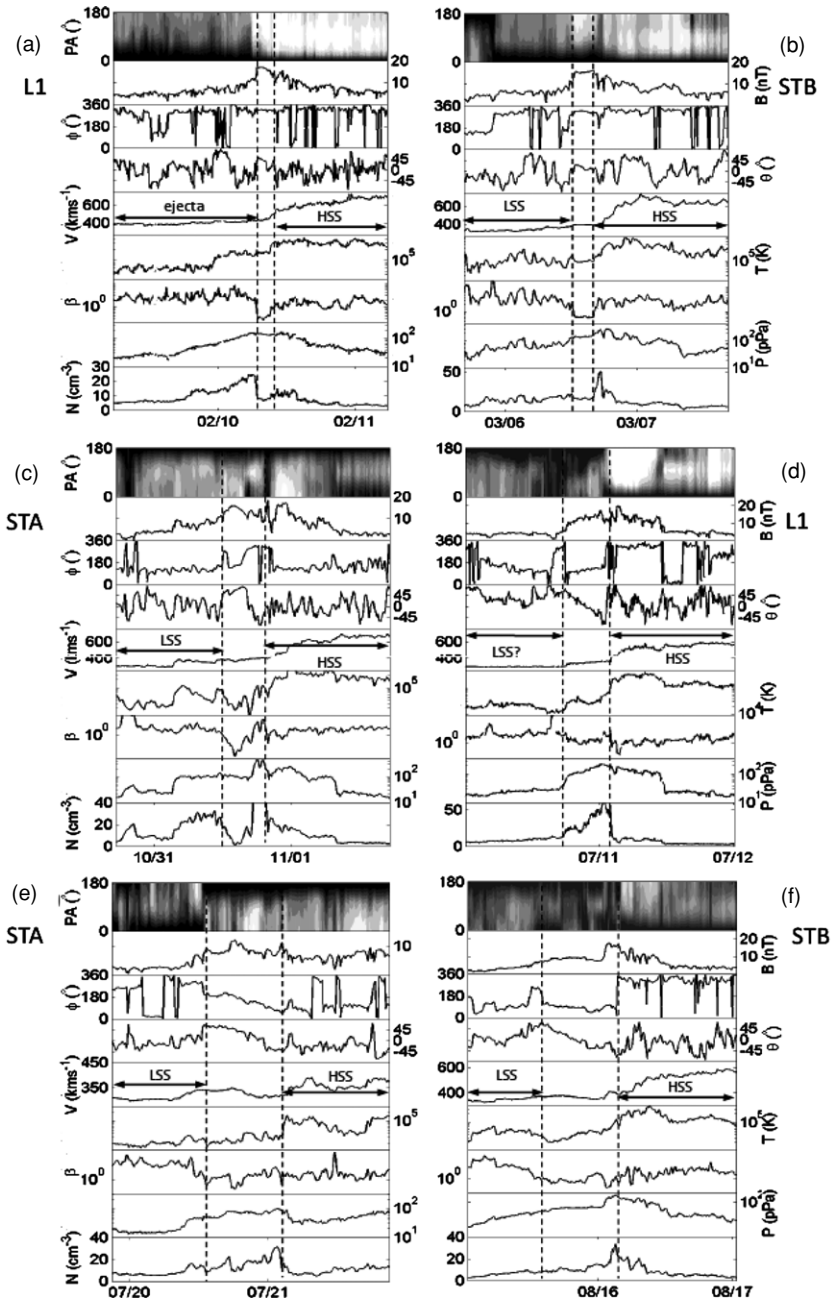

Figure 1. In situ measurements made by the L1 (*ACE*/*Wind*) (a, d), *STA* (c, e), and *STB* (b, f) spacecraft of six transient events. A nine-panel plot is presented for each event. The top panel of each plot presents pitch angle spectrograms of 272 eV electrons measured by *ACE* (a, d) and equivalent spectrograms for 250 eV electrons measured by *STEREO* (a, b, e, f). High and low fluxes appear as black and white areas, respectively. The remaining eight panels in each plot present in descending order: the strength (B (nT)), azimuth ($\phi(^\circ)$), and elevation angles ($\theta(^\circ)$) of the interplanetary magnetic field, the proton speed (V (km s^{-1})), proton temperature (K), plasma beta (β), total perpendicular pressure (P (nPa)), and proton density (N (cm^{-3})) of solar wind protons. The intervals of transient passages are bound by dotted lines, the times of passage of low-speed stream (LSS), and high-speed stream (HSS) are also shown.

Table 1
Properties of the Small-scale Transients Measured In Situ

T_S	T_E	ΔT	V	ΔR	β	In Situ	HI
2008 Feb 10 06:46	2008 Feb 10 09:12	$2^h22'$	430	0.025	0.3	L1	N/A
2008 Mar 6 12:23	2008 Mar 6 16:19	$3^h55'$	386	0.037	0.9	*STB*	N/A
2008 Oct 31 12:39	2008 Oct 31 17:30	$4^h55'$	375	0.049	0.1	*STA*	*STB*
2007 Jul 10 18:00	2007 Jul 11 01:43	$7^h18'$	345	0.064	0.95	L1	*STB*
2007 Jul 20 12:48	2007 Jul 21 01:37	$12^h10'$	330	0.102	<0.8	*STA*	*STB*
2008 Aug 15 13:41	2008 Aug 16 03:00	$13^h18'$	368	0.118	<0.9	*STB*	*STA*

Note. The start time ($T_S(UT)$), end time (T_E(UT)), duration of the event (ΔT(s)), speed (V (km s^{-1})), spatial extent (ΔR (AU)), plasma beta parameter (β), in situ spacecraft where the measurements were made, and the spacecraft that could potentially have detected the white-light signature.

the transients shown in Figure 1. The bi-directional electrons observed near sudden changes in total pressure are more likely to result from back-streaming electrons accelerated at shocks further out in the solar wind (Steinberg et al. 2005; Lavraud et al. 2010) rather than electrons bi-streaming on closed magnetic field lines (Gosling et al. 1987). All these events were slow ($<$450 km s^{-1}) and occurred, as required, just prior to the arrival of HSSs.

The two transients presented in Figures 1(a) and (b) have remarkably small radial extents ($<$0.05 AU) and are marked by sharp decreases in plasma β values. Their sizes are nearly an order of magnitude smaller than magnetic flux ropes traditionally reported in the literature. The period that precedes the arrival of the small transient event on February 10, shown in Figure 1(a), is associated with the passage of plasma with high alpha to proton ratio (not shown here) and is the transient associated with the CME observed by Wood et al. (2009).

All of the events shown in Figure 1 are associated with peaks in plasma densities exceeding 20 cm^{-3} inside the interaction region where the total perpendicular pressure is normally enhanced. These enhanced pressures and densities are associated with an HSS compressing the small transients. This compression is analogous to the compression of low-speed streams (LSS) inside corotating interaction regions (CIRs). In the next sections, we investigate whether plasma density increases are observed by the white-light imagers. In such cases, we investigate the solar origin of these small transients by using the white-light signal to follow the transient back to the Sun.

3. SMALL INTERPLANETARY TRANSIENTS (0.05–0.12 AU) TRACED BACK TO CMEs

The transients shown in Figures 1(c) and (f) were observed near 1 AU in the white-light images taken by the Heliospheric Imager (HI) component of the *SECCHI* package. *SECCHI*, on each *STEREO* spacecraft, consists of an Extreme Ultraviolet Imager (EUVI), two coronagraphs (COR-1 and COR-2), and two HI cameras. The combined *SECCHI* cameras allow us to track transients continuously from the Sun to 1 AU. The wide field, wide angle HI cameras are described in detail by Eyles et al. (2009) and Brown et al. (2009).

The tracks made in J-maps by the four largest transients, presented in Figures 1(c)–(f), were continuous and could be followed back to the Sun. The J-maps, in this case, are constructed by extracting the intensity variation in a band of pixels distributed along a constant position angle from a series of COR-2 and HI-1/2 composite running-difference images, and plotting this variation as a function of elongation (*Y*-axis) and time (*X*-axis) (Sheeley et al. 1999; Davies et al. 2009). A J-map constructed from combined COR-2, HI-1/2 images taken by *STB* is shown in Figure 2(a). The elongation variation of the *STA* spacecraft measuring the transient in situ is plotted as a near-horizontal white line.

Transients can appear to accelerate/decelerate rapidly at the elongations imaged by the HI instruments; this is largely an effect of geometry (Rouillard et al. 2008, 2009a, 2009b; Sheeley et al. 2008a, 2008b). The elongation variation with time, $\alpha(t)$, of a point in the solar wind depends upon its radial speed, V_r, and its angle of propagation out of the sky plane δ (or equivalently $\beta = 90^\circ - \delta$):

$$\tan(\alpha(t)) = \frac{V_r t \cos \delta}{r_{A/B} - V_r t \sin \delta}, \quad (1)$$

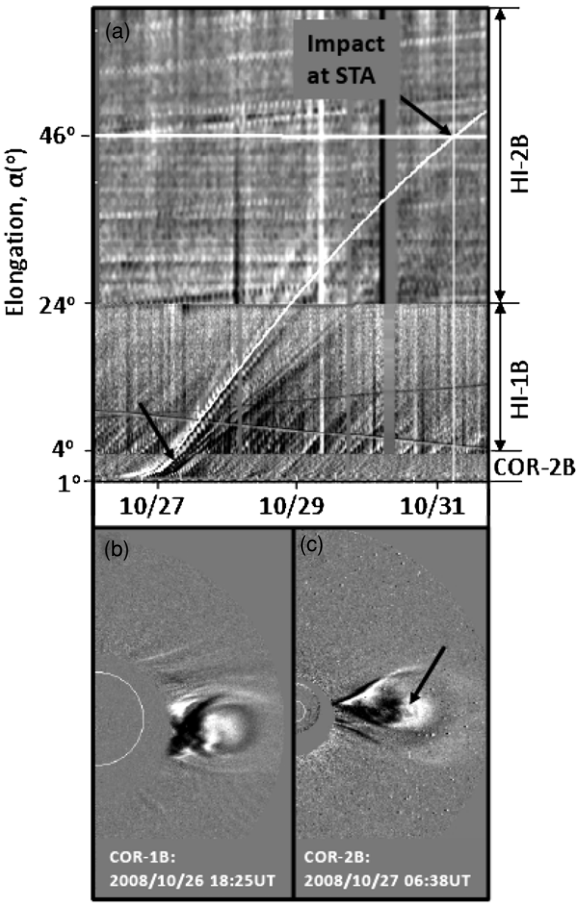

Figure 2. White-light observations of a CME observed by *STEREO* in 2008 October 26–31. A J-map, created using running-difference images from the COR-2, HI-1, and HI-2 instruments onboard *STB* (a). The elongation variation calculated from the corresponding in situ measurements is overplotted as a white curve and the time of impact is shown. The COR-1 (b) and COR-2 (b) running-difference observations of the CME are also shown. Black arrows point to the sections of the CMEs observed in the images and to the corresponding signature in the J-map.

where $r_{A/B}$ is the radial distance of the observing spacecraft (*STA* or *STB*). Values of δ and V_r can be obtained from fitting to the elongation variation of the transient recorded by HI, thereby providing an estimated trajectory and velocity for the transient. Conversely, knowledge of the time of impact and speed of a transient measured in situ by a spacecraft located at an angle of δ out of the sky plane can be used to compute the expected elongation variation, $\alpha(t)$.

The computed $\alpha(t)$ of the transient detected in situ on 2008 October 31 at *STA* (Figure 1(c)) is plotted as a white curve superposed on the J-map shown in Figure 2(a). This calculated trajectory passes through a set of diverging tracks. Each of these observed tracks is associated with a density structure transported by a large bulb-shaped CME, initially observed in COR-1/2B on 2008 October 27 (Figures 2(b) and (c)). The *STEREO* measurements have shown that large CMEs with trajectories directly aimed at in situ spacecraft are usually associated with extended flux ropes ($>$0.15 AU) (Rouillard et al. 2009b, 2010a, 2010c; Möstl et al. 2009; Davis et al. 2009; Kilpua et al. 2009a), yet we find here a case of a small transient that traces back to a major CME event. The CME launch is marked with a sudden release of dense material observed by the EUVI instruments on *STA* and *STB* at 284 Å and 197 Å, and the transit of the CME is clearly observed in the lower field of view of the COR-1B

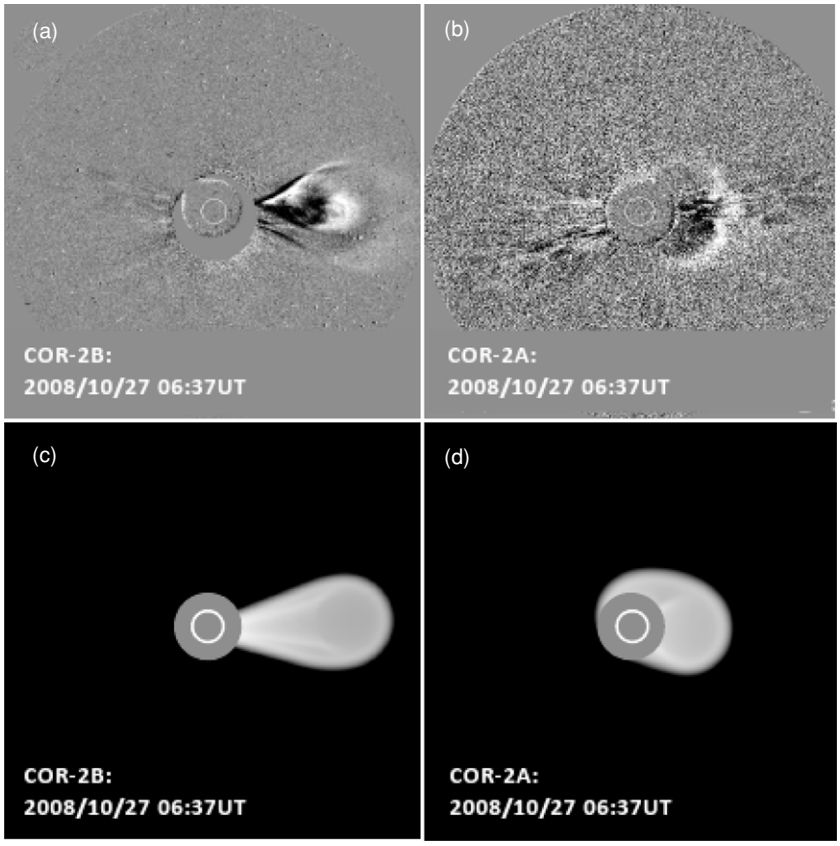

Figure 3. COR-2B (a) and COR-2A (b) running-difference images showing the eruption of the 2008 October 26–31 CME which impacted *STA* (Figure 1(c)). Two white-light simulation results, using the Thernisien et al. model and showing the total brightness of the CME as viewed from COR-2B (c) and COR-2A (d).

instrument (Figure 2(b)). We can also calculate the trajectory of the CME by fitting the J-map tracks independently of the in situ measurements (e.g., Rouillard et al. 2010a); doing so we find that the density enhancement located on the front of the CME and observed by HI on *STB* is propagating some 10° west of the Sun–*STA* line.

The CME was observed off the west limb of the Sun in COR-2B images (Figure 3(a)) but in COR-2A images the density variations are also mostly visible off the west limb (i.e., a partial Halo CME; Figure 3(b)). This latter observation suggests that the central axis of the CME was not propagating exactly along the Sun–*STA* line but slightly more westward. The CME outline is well defined in these running-difference images, we therefore use the white-light rendering technique of Thernisien et al. (2006) to investigate the three-dimensional orientation of the magnetic flux rope. The results of simulating the white-light images are shown in Figures 3(c) and (d), for COR-2B and COR-2A, respectively. According to this simulation, a best fit is obtained for a nearly horizontal flux rope with its central axis located 13° westward of *STA*; therefore, *STA* passed through the eastern edge of the CME probably intersecting a small section of the magnetic flux rope. The small extent of the magnetic structure could be related to *STA* only grazing a large magnetic flux rope. This hypothesis is discussed in the last section.

The small transients measured in situ by *STB* on 2008 August 18 (Figure 1(f)) could also be traced back to the Sun by using a J-map (Figure 4(a)), combined with knowledge of the elongation variation of the in situ observer. This small structure is traced back to the back end of a well-defined CME eruption observed off the east limb of the Sun by COR-2A (Figure 4(c)). This CME was smaller than the 2008 October 27 event and did

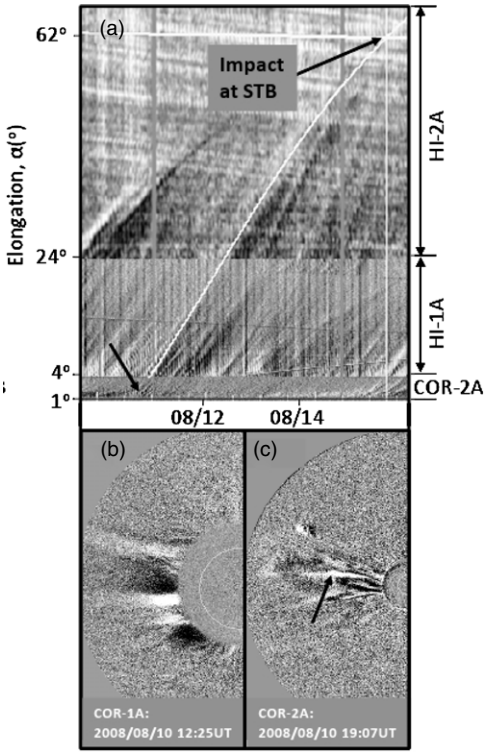

Figure 4. Same format as Figure 2 but for the 2008 August event (Figure 1(f)) observed in white light by *STA* and measured in situ by *STB*.

not contain a clear cavity, but rather loop-like features observed by COR-2A. The passage of the CME was also detected in

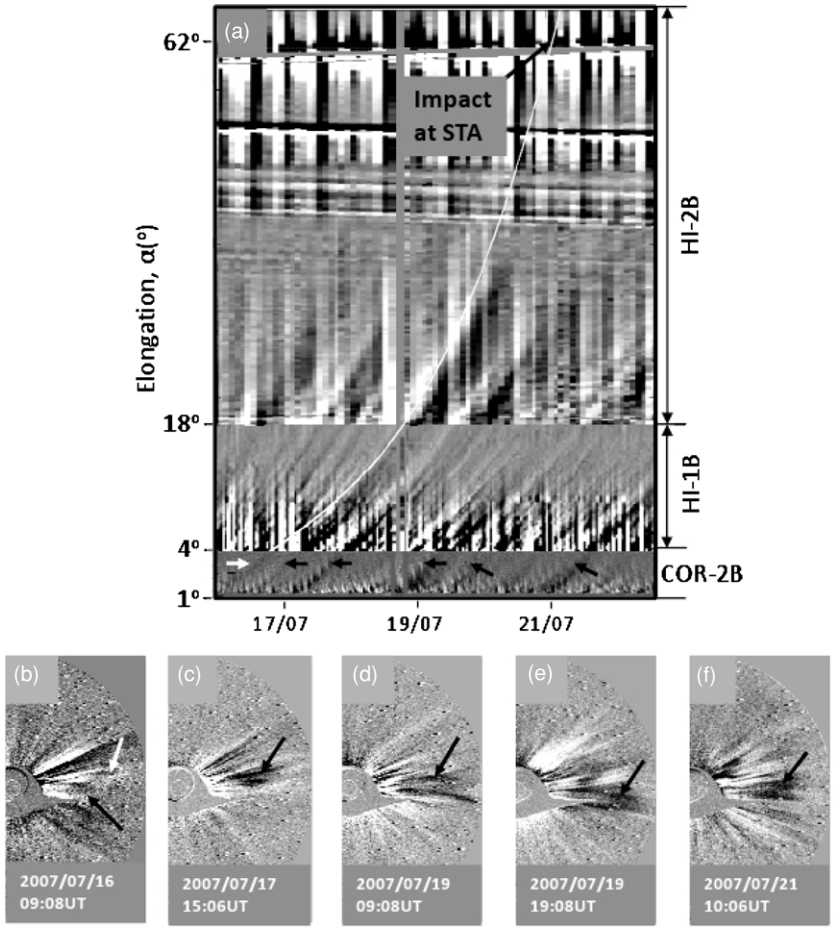

Figure 5. J-map constructed from *STB* observations taken during the 2007 July 16–22 time interval. This J-map is presented in the same format as the one shown in Figure 2(a). The COR-2B section of the J-map was stretched in elongation to facilitate the tracking of the individual streamer arches. Panels (b)–(f) present COR-2B running-difference images for each transient outflow shown in the COR-2B section of the J-map. One of the two small transients observed in panels (b) and (c) is associated with the small transient measured in Figure 1(e).

the COR-1A field of view as poorly resolved density variations (i.e., $< 2\,R_{\odot}$) (white features in Figure 4(b)). The expected elongation variation of the dense part of the ejection matches the track observed in the J-map (Figure 4(a)). We must therefore conclude that the CME propagation path was aligned along the Sun–*STB* line. In this case, the small size of the transient measured in situ is more likely related to the actual small size of the CME event observed in white light (Figure 2(e)). This narrow CME event is probably analogous to the class of small CMEs described by Gilbert et al. (2001).

These are two examples of small transients detected in situ tracing back to a small and a large CME, both of which are associated with density variations in the very inner corona (i.e., in COR-1 images). In the next section, we find that small transients can also trace back to density variations associated with the outflow of density structures that appear as narrow CMEs and "arch-like structures" in COR-2 images but which produce either no or else very faint density variations in COR-1 images.

4. SMALL INTERPLANETARY TRANSIENTS (0.05–0.12 AU) TRACED BACK TO STREAMER EVENTS

The white-light signature of the small magnetic cloud shown in Figure 1(e) is discussed in detail by Rouillard et al. (2009a) and consisted of a well-defined large-scale wave propagating in HI-1/2B at an angle $\delta \sim 73^{\circ}$ out of the plane of the sky. It was interpreted as being the signature of an interaction region that developed between the small magnetic cloud measured in situ (Figure 1(e)) and the HSS that follows. This wave leaves a continuous track in J-maps constructed from COR-2 and HI running-difference images (Figure 5(a)). Rouillard et al. (2009a) did not investigate the solar origin of this event in COR-2B images, now shown in Figures 5(b)–(f). The wave traces back to a part of the lower corona where very small ejecta appear to erupt continually along streamer rays. A careful inspection of the COR-2 running-difference images and the associated portion of the J-map shown in Figure 5(a) reveals that at least two small ejecta (white and black arrow in Figure 5(a)), one of which has the appearance of a small loop, erupted and merged to form the main track associated with the small magnetic cloud measured in situ (Figure 1(e)). These ejecta are very faint in COR-2B and are undetected by COR-1B.

This merging is probably not real but rather the result of the alignment, along the lines of sight in the HI-1/2B field of view, of the two structures that are propagating at slightly different longitudes. It has been shown, mathematically, that transients propagating at small angles ($<20^{\circ}$) relative to *STB* and expelled successively by the same corotating source region (and therefore propagating along slightly different longitudes but lying on the same spiral) will appear from *STB*'s perspective to be aligned for most of their transit to 1 AU (Sheeley & Rouillard 2010). The temporal and spatial proximity of these two small eruptions prevent us from determining from *STB* images alone which

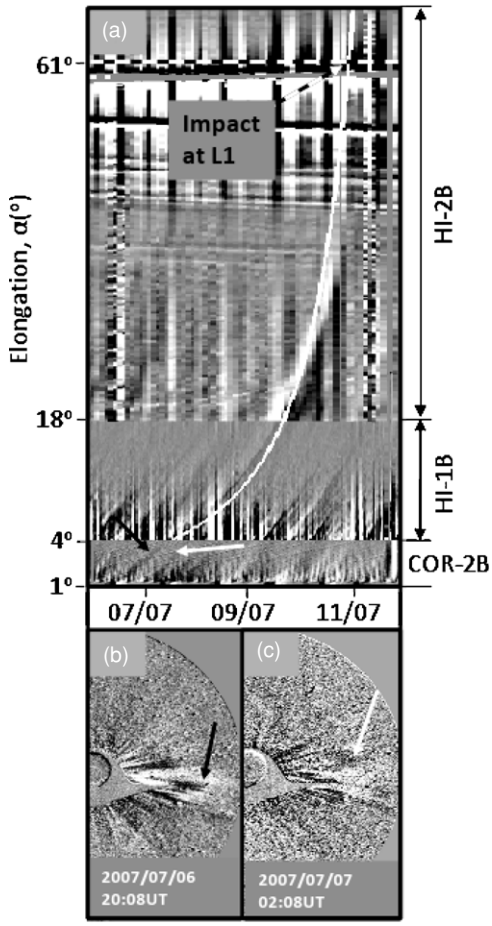

Figure 6. Similar format as Figure 2 but here showing the outflow of two small transients observed in COR-2B running-difference images (b, c) and tracked to the L1 Lagrange point using an *STB* J-map (a). Black and white arrows mark the position of the two transients in the COR-2B images and in the corresponding section of the J-map. One of these two small transients is associated with the small transient measured in Figure 1(d).

of the two streamer structures was associated with the small magnetic cloud detected near 1 AU (Figure 1(e)).

These streamer ejecta are not as clearly detected in COR-1 images and may be analogous to the face-on views of streamer blobs which appear to form beyond 3–4 $R_{\odot}$ (Sheeley et al. 2009). Figure 5(e) offers a clearer example of one of these ejecta that erupted off the west limb on July 19. Figures 5(c)–(f) show that the eruption of small ejecta can last for several days and that they are the origin, in the lower corona, of the diverging tracks observed during this period in the HI-2B field of view. These diverging tracks are well-known signatures of the presence of CIRs where transients are compressed ahead of the fast solar wind (e.g., Sheeley & Rouillard 2010).

The transient signature measured at the L1 Lagrange point on 2007 July 10 (Figure 1(d)) was also traced back to a period of released ejecta. Figure 6(a) presents the J-map associated with these events. Again, two ejecta merge in the lower corona to form the main track, the second of these ejecta appears as a poorly defined arch-like structure. The elongation variation calculated from the speed and arrival time of the transient detected at L1 is again overplotted on this J-map. We suggest that one of these two small ejecta, which appear to merge to form the main track, is propagating along the Sun–Earth line but the vantage point offered by *STB* does not allow us to determine which of the two is associated with the magnetic field rotation measured in situ.

5. THE ORIGIN OF A VERY SMALL TRANSIENT (<0.05 AU)

The smallest magnetic transients that we could identity in situ were shown in Figures 1(a) and (b). Unfortunately, neither of these two transients produced a continuous track in J-maps that could be used to investigate their solar origin. Figure 1(a) presented the smallest of the two structures. We used a ballistic back-mapping method, based on the speed and arrival time of the transient at L1 (but without the J-map analysis) to estimate the launch time of this structure. We found that it could have originated from a very well-defined arch observed by COR-2B on 2008 February 5 at 18UT. However, without it producing a continuous track in the J-map, there is no way of knowing if the arch-like structure was indeed propagating toward L1. It appears that the origin of the smallest of magnetic field rotations (<0.05 AU) may prove difficult to determine using a J-map analysis of *SECCHI* observations.

6. TRACKING ARCHES TO 1 AU: A CASE OF A MAGNETIC FIELD REVERSAL

The combined J-map and back-mapping procedure employed so far in this paper has revealed an association between poorly defined ejecta and magnetic features which may be magnetic flux ropes. In the last section of this paper, we approach the problem the opposite way; we find a well-defined example of an erupting arch-like structure that is predicted to propagate toward a spacecraft making in situ measurements. This analysis provides the first direct association between a magnetic field reversal of the kind described by Crooker et al. (1996b) and a streamer arch observed in white-light images. Unlike the previous events, no smooth magnetic field rotation is associated with this event, however its short duration (<12 hr) and its association with erupting streamer arches make its analysis directly relevant to the present study.

Figure 7(a) shows the J-map associated with the outflow of two well-defined arches on 2008 June 21; this is the same event described in Figure 10 of Sheeley & Rouillard (2010). These arches were observed by COR-2B and appear to merge to form a continuous track in HI-1B, the first of a set of diverging tracks. This divergence of tracks suggests that HSSs are once again sweeping up these arch-like structures between the Sun and 1 AU. Figures 7(b) and (c) show the two arch-like structures transiting successively through the COR-2B field of view. The three-dimensional trajectory of the small-scale transient was obtained by fitting the observed track in the manner of Rouillard et al. (2010b). The best-fit curve is overplotted on the J-map. We find that the trajectories of these arches are directed within a 5° angle of the Sun–L1 line.

The in situ measurements taken at L1 at the predicted time of impact are shown in Figure 8. The arrival of a CIR is measured at the predicted time of impact of the white-light transient. The CIR passage is associated with elevated solar wind density (>30 cm^{-3}) followed by a hotter fast solar wind. No transient with the properties defined in Section 2 is observed at the time; the plasma beta remains greater than 1 and there is no smooth rotation of the magnetic field. A few hours before the HSS arrival *ACE*/*Wind* detect a true sector boundary (SB) marked by a sudden change of electron pitch angles from 180° to 0°, with no clear heliospheric current sheet crossing (Figures 8(c) and (d)) but a first density increase associated with the arrival of the CIR (Figure 8(i)). This current sheet is located inside a region of high density (Figure 8(i)). Immediately after the passage of the first

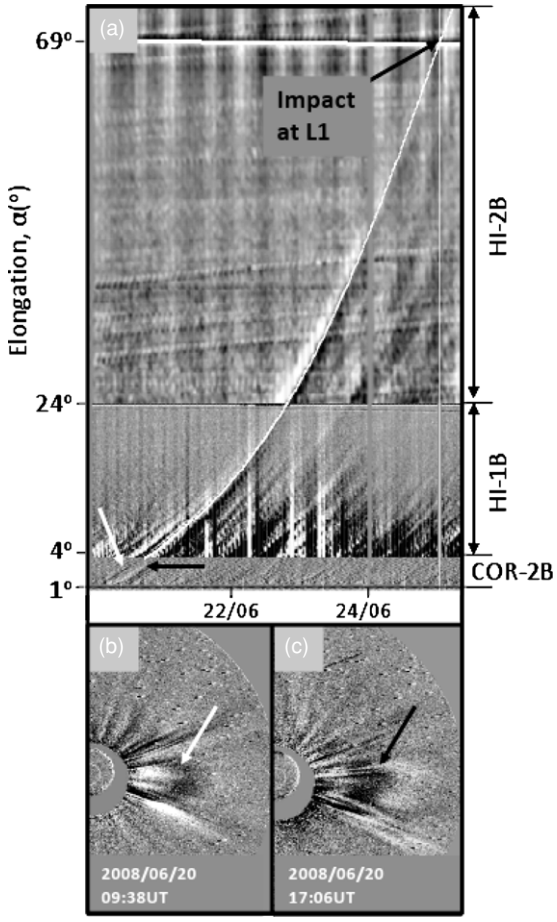

Figure 7. Same format as Figure 2. These white-light observations were made during the 2008 June 20–25 time interval. Two very well-defined streamer arches are tracked continually from COR-2B to the L1 Lagrange point using HI-1B and HI-2B observations. One of the two transients shown in panels (b) and (c) is associated with the in situ measurements of a transient shown in Figure 7.

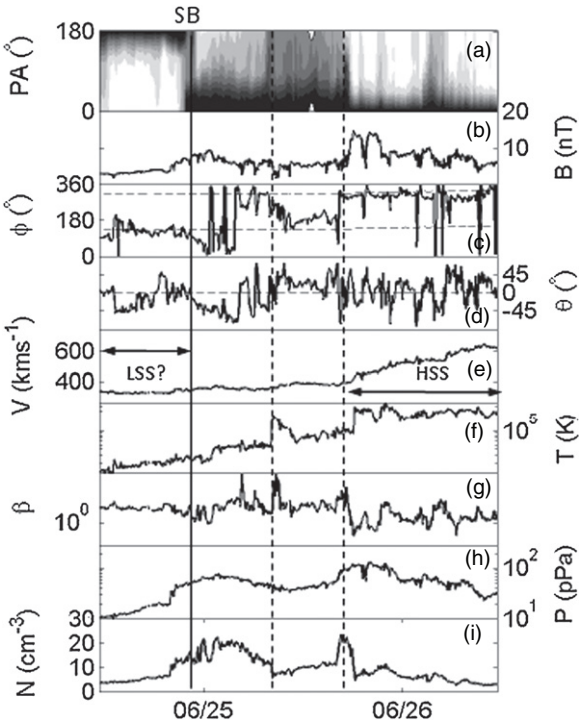

Figure 8. In situ measurements made by the *ACE*/*Wind* spacecraft at the L1 Lagrange point between 2008 June 24 12:00UT and June 26 12:00UT, and presented in the same format as Figure 1. The occurrence of the magnetic field inversion is bound by two dotted lines. The location of the true section boundary (SB) is also shown.

high plasma density structure, the magnetic field switches back to the orientation prior to the current sheet crossing and keeps this orientation for a period of several hours. This change of magnetic field direction from outward to inward is not expected from an examination of the suprathermal electron data shown in Figure 8(a); the pitch angles of these particles, which should have switched back to 180° with the reversal of the magnetic field vector, remain at 0° throughout this interval. A second density peak marks the end of this anomalous period.

Changes of the magnetic field direction of 180° that are not associated with corresponding changes in the pitch angles of suprathermal electrons have been associated with large kinks in the magnetic field lines (Crooker et al. 1996a, 1996b). These turnings are thought to result from the grazing of transient structures, such as magnetic flux ropes (Baker et al. 2009) or so-called refolded magnetic field lines (Crooker et al. 1996a). In both cases, the magnetic field lines are connected to the Sun at one end only, but the spacecraft intersects a section of the magnetic field line that is temporarily oriented in the opposite direction to the Parker spiral orientation expected from the pitch angle data. This structure is bounded by dotted lines in Figure 8, is located between the first and second density increase, and is embedded within the CIR. The J-map track links these measurements to the two arch-like structures observed by COR-2B (Figures 7(b) and (c)). We associate the transient signature measured in situ in Figure 8 directly with the passage of one of these arch-like structures. These observations suggest that arch-like structures are not necessarily associated with a smooth magnetic field rotations but can be complicated structures, perhaps associated with local kinks in the magnetic field lines.

7. DISCUSSION AND CONCLUSION

Previous studies have shown that large CMEs continuously tracked to 1 AU are often associated with smooth rotations of the magnetic field extending over radial distances greater than 0.15 AU (e.g., see the review by Rouillard et al. 2011). In the present paper, we started with the identification in situ of short magnetic field rotations extending over ∼0.025– ∼0.118 AU. J-maps were subsequently used to investigate their solar origin. We could not determine if the smallest in situ transients (Figures 1(a) and (b)) were magnetic flux ropes, nor could we successfully track their solar origin.

We have found several origins for the rotations of the magnetic field vector extending over 0.05–0.118 AU. One of these small magnetic transients (Figure 1(c)) was traced back to a major CME eruption with a bulb shape that is reminiscent of a large magnetic flux rope. A white-light rendering technique provided strong evidence that the CME central axis was not directed at the spacecraft and that, in consequence, the in situ measurements were made on the periphery of the magnetic flux rope; the small size of the transient is, we think, a consequence of missing most of the magnetic fields of this CME. Another short magnetic field rotation (Figure 1(f)) could be traced back to a CME that was smaller than the October 27 event, but that had a detectable signature in COR-1 images. Finally, two magnetic field rotations (Figures 1(d) and (e)) could be traced back to poorly defined ejecta which occasionally appear as arches in COR-2 images.

We therefore conclude that small transients in the solar wind can result from the following.

1. Grazing of CMEs which outlines that are reminiscent of the geometry of magnetic flux ropes. These large CMEs are already apparent below helmet streamers with signatures in the entire COR-1 field of view.
2. Small and narrow CMEs with no "bulb- or bubble-shaped" outline but which erupt from the lower corona well below helmet streamers, they may be analogous to the narrow CMEs reported by Gilbert et al. (2001).
3. Poorly defined, often narrow, ejecta that are not associated with chromospheric activity and only become resolved in the COR-2 field of view. These ejecta occasionally appear as arches in running-difference image and may be analogous to the streamer arches reported by Sheeley et al. (2009).

It is not immediately obvious how the grazing of a large CME flux rope could be measured as a short rotation of the magnetic field vector. Indeed, a spacecraft grazing the eastern or western boundary of a "croissant-shaped" flux rope located in the ecliptic and with its central axis parallel to the ecliptic plane should intuitively pass through the "legs" of the flux rope as well (thereby leading to a long rotation of the magnetic field). These "legs" are even more poorly understood than the leading edges of CMEs and assumptions on their geometry are still highly speculative. However, in cases where CMEs are compressed by HSSs, we can reasonably expect that the magnetic field lines joining the leading edge of the CME to the Sun are forced to corotate due to the high pressures induced by the compressive effects of the HSS. In such a case, the in situ observer intersects the eastern edge of the flux rope and, instead of passing through the "legs" of the CME, enters immediately into the HSSs that follow. Such a scenario could have been encountered by *STA* for the event presented in this paper (Figure 1(c)), but also at *STB* in 2007 November (Farrugia et al. 2011; see also diagram in Figure 4 of Rouillard et al. 2010c).

The near-absence in COR-1 images of the poorly defined narrow ejecta could be a result of the sensitivity of the camera but another possibility is that the physical phenomena associated with their formation and outflow only lead to significant density variations beyond the COR-1 field of view. Sheeley et al. (2009) showed that many arch-like structures are the face-on views of the well-known "streamer blobs." The blobs were found in the LASCO C2 coronagraph, to form near the tip of helmet streamers beyond 3–4 $R_{\odot}$ (just beyond COR-1) (Sheeley et al. 1997). It is therefore likely that the arches presented in this paper also form near the tip of helmet streamer. We note that some arches could be forming even higher up in the atmosphere in the COR-2 field of view (6–12 $R_{\odot}$) where the plasma beta remains low and reconnection between oppositely directed magnetic field lines is likely (Gosling et al. 2006; Phan et al. 2010).

The nature of small rotations in the interplanetary magnetic field data has been controversial and is closely related to the origin and properties of the slow solar wind. Feng et al. (2008) suggested that all magnetic flux ropes measured in situ are the results of CMEs. Arch-like structures appear to be small versions of CMEs; however, unlike many CMEs, no filament activity is observed in EIT images during their eruptions and they typically appear above the cusp of helmet streamers in the outer portion of the COR-1 field of view (Sheeley et al. 2009). The large number of transient eruptions observed above helmet streamers is strongly suggestive that the slow solar wind convects a significant number of these transient structures. Our study shows that a whole spectrum of CMEs carrying short magnetic field rotations erupt from the chromosphere and the lower corona and may be forming at different heights.

We have found a case where two very similar arches erupted in the COR-2 field of view and formed a continuous track in HI-1/2 J-maps. The associated in situ measurements revealed the presence of a temporary reversal of the magnetic field direction without a change in the magnetic field polarity. The origin of such structures has previously been associated with the reconnection of open and closed magnetic field lines near the Sun (Crooker et al. 2004) or to erupting magnetic flux ropes reconnecting with open magnetic field lines (Baker et al. 2009).

Various models developed to describe the transport of magnetic field lines on the Sun invoke reconnection between open and closed magnetic field lines to enable a dynamical relaxation of the coronal magnetic field (Wang et al. 2008; Fisk & Schwadron 2001; Owens et al. 2007; Lavraud et al. 2011). Is this type of reconnection associated with the release of small ejecta? Rouillard et al. (2010c) presented in situ measurements of bi-directional streaming electrons located inside a magnetic flux-rope that had been entrained by an HSS. These closed magnetic field lines were traced back, using J-maps, to the outflow of poorly resolved streamer ejecta observed in COR-2 images. Additionally, Kilpua et al. (2009a) presented evidence for the presence of numerous transients associated with bi-directional suprathermal electrons embedded in the slow solar wind during 2007–2008. It is therefore likely that poorly defined events are, on occasions, associated with the release of closed loops measured in situ as smooth magnetic field rotations but which do not reconnect with open magnetic field lines. Reconnection between open and closed field lines may therefore not be necessary for the release of poorly defined events in general.

The main difficulty faced in the present study has been associated with the observations of the details of streamer arches and other poorly defined ejecta. This is related to their associated weak density fluctuations and the large distance that separates the lower corona and the *STEREO* spacecraft. These observations stress the importance of future missions such as the Solar Orbiter and Solar Probe Plus missions which will enable more detailed observations of these ejecta by recording white-light images much closer to the Sun.

The *STEREO*/*SECCHI* data are produced by a consortium of *RAL* (UK), *NRL* (USA), *LMSAL* (USA), *GSFC* (USA), *MPS* (Germany), *CSL* (Belgium), *IOTA* (France), and *IAS* (France). The *ACE* data were obtained from the *ACE* science center. The *Wind* data were obtained from the *Space Physics Data Facility*. The *SECCHI* images were obtained from the Naval Research Laboratory, Washington DC, USA, and the World Data Center, Chilton, UK. This work was partly supported by NASA. E.K.J.K.'s study was supported through the Academy of Finland (project 130298). The NRL employees acknowledge support from the Office of Naval Research. The work of A.P.R. was partly funded by NASA contracts NNX11AD40G-45527 and NNXIOAT06G.

REFERENCES

Baker, D., et al. 2009, Ann. Geophys., 27, 3883
Belcher, J. W., & Davis, L., Jr. 1971, J. Geophys. Res., 76, 3534
Bothmer, V. 2003, in Solar Variability as an Input to the Earth's Environment, ed. A. Wilson (ESA SP-535; Noordwijk: ESA), 419
Bothmer, V., & Schwenn, R. 1998, Ann. Geophys., 16, 1
Brown, D. S., Bewsher, D., & Eyles, C. J. 2009, Sol. Phys., 254, 185

Burlaga, L. F., Berdichevsky, D., Gopalswamy, N., Lepping, R., & Zurbuchen, T. 2003, J. Geophys. Res., 108, 1425
Burlaga, L. F., Sittler, E., Mariani, F., & Schwenn, R. 1981, J. Geophys. Res., 86, 6673
Cartwright, M. L., & Moldwin, M. B. 2008, J. Geophys. Res., 113, A09105
Chen, J., et al. 1997, ApJ, 490, L191
Crooker, N. U., Burton, M. E., Phillips, J. L., Smith, E. J., & Balogh, A. 1996a, J. Geophys. Res., 101, 2467
Crooker, N. U., Burton, M. E., Siscoe, G. L., Kahler, S. W., Gosling, J. T., & Smith, E. J. 1996b, J. Geophys. Res., 101, 24331
Crooker, N. U., Kahler, S. W., Larson, D. E., & Lin, R. P. 2004, J. Geophys. Res., 109, A03108
Davis, C. J., Davies, J. A., Lockwood, M., Rouillard, A. P., Eyles, C. J., & Harrison, R. A. 2009, Geophys. Res. Lett., 36, L08102
Davies, J. A., et al. 2009, Geophys. Res. Lett., 36, L02102
Démoulin, P., & Dasso, S. 2009, A&A, 498, 551
Eyles, C. J., et al. 2009, Sol. Phys., 254, 387
Farrugia, C. J., et al. 2011, J. Atmos. Sol. Terr. Res., in press
Feng, H. Q., Wu, D. J., Lin, C. C., Chao, J. K., Lee, L. C., & Lyu, L. H. 2008, J. Geophys. Res., 113, A12105
Fisk, L. A., & Schwadron, N. A. 2001, ApJ, 560, 425
Galvin, A. B., Kistler, L. M., Popecki, M. A., Farrugia, C. J., Simunac, K. D. C., & Ellis, L. 2008, Space Sci. Rev., 136, 437
Gilbert, H. R., Serex, E. C., Holzer, T. E., MacQueen, R. M., & McIntosh, P. S. 2001, ApJ, 550, 1093
Gloeckler, G., et al. 1998, Space Sci. Rev., 86, 497
Gosling, J. T., Baker, D. N., Bame, S. J., Feldman, W. C., Zwickl, R. D., & Smith, E. J. 1987, J. Geophys. Res., 92, 8519
Gosling, J. T., Birn, J., & Hesse, M. 1995, Geophys. Res. Lett., 22, 869
Gosling, J. T., McComas, D. J., Skoug, R. M., & Smith, C. W. 2006, Geophys. Res. Lett., 33, L17102
Gosling, J. T., Teh, W.-L., & Eriksson, S. 2010, ApJ, 719, L36
Howard, R. A., Sheeley, N. R., Jr., Michels, D. J., & Koomen, M. J. 1985, J. Geophys. Res., 90, 8173
Howard, R. A., et al. 2008, Space Sci. Rev., 136, 67
Issautier, K., Perche, C., Hoang, S., Lacombe, C., Maksimovic, M., Bougeret, J.-L., & Salem, C. 2005, Adv. Space Res., 35, 2141
Kilpua, E. K. J., et al. 2009a, Sol. Phys., 256, 327
Kilpua, E. K. J., et al. 2009b, Ann. Geophys., 27, 4491
Klein, L. W., & Burlaga, L. F. 1982, J. Geophys. Res., 87, 613
Lavraud, B., Owens, M., & Rouillard, A. P. 2011, Sol. Phys., in press
Lavraud, B., et al. 2010, Ann. Geophys., 28, 233
Lepping, R. P., Wu, C.-C., Berdichevsky, D. B., & Ferguson, T. 2008, Ann. Geophys., 26, 1919
Lepping, R. P., et al. 1995, Space Sci. Rev., 71, 207
Lin, R. P., et al. 1995, Space Sci. Rev., 71, 125
Liu, Y., Richardson, J. D., & Belcher, J. W. 2005, Planet. Space Sci., 53, 3
Luhmann, J. G., et al. 2008, Space Sci. Rev., 136, 117
Marubashi, K. 1986, Adv. Space Res., 6, 335
Marubashi, K. 1991, Adv. Space Res., 11, 57
Marubashi, K., Cho, K.-S., & Park, Y.-D. 2010, in AIP Conf. Proc. 1216, 12th International Solar Wind Conference, ed. M. Maksimovic et al. (Melville, NY: AIP), 240
McComas, D. J., Bame, S. J., Barker, P., Feldman, W. C., Phillips, J. L., Riley, P., & Griffee, J. W. 1998, Space Sci. Rev., 86, 563
Möstl, C., Farrugia, C. J., Temmer, M., Miklenic, C., Veronig, A. M., Galvin, A. B., Leitner, M., & Biernat, H. K. 2009, ApJ, 705, L180
Newbury, J. A., Russell, C. T., Phillips, J. L., & Gary, S. P. 1998, J. Geophys. Res., 103, 9553
Ogilvie, K. W., et al. 1995, Space Sci. Rev., 71, 55
Owens, M., et al. 2007, Geophys. Res. Lett., 34, 06104
Phan, T. D., et al. 2010, ApJ, 719, L199
Rouillard, A. P. 2011, J. Sol. Terr. Atmos. Res., in press
Rouillard, A. P., Lavraud, B., Sheeley, N. R., Davies, J. A., Burlaga, L. F., Savani, N. P., Jacquey, C., & Forsyth, R. J. 2010a, ApJ, 719, 1385
Rouillard, A. P., et al. 2008, Geophys. Res. Lett., 35, L10110
Rouillard, A. P., et al. 2009a, Solar Phys., 256, 307
Rouillard, A. P., et al. 2009b, J. Geophys. Res., 114, A07106
Rouillard, A. P., et al. 2010b, J. Geophys. Res., 115, A04103
Rouillard, A. P., et al. 2010c, J. Geophys. Res., 115, A04104
Sauvaud, J.-A., et al. 2008, Space Sci. Rev., 136, 227
Sheeley, N. R., Jr., Lee, D. D.-H., Casto, K. P., Wang, Y. -M., & Rich, N. B. 2009, ApJ, 694, 1471
Sheeley, N. R., Jr., & Rouillard, A. P. 2010, ApJ, 715, 300
Sheeley, N. R., Jr., Walters, J. H., Wang, Y.-M., & Howard, R. A. 1999, J. Geophys. Res., 104, 24739
Sheeley, N. R., et al. 1997, ApJ, 484, 472
Sheeley, N. R., Jr., et al. 2008a, ApJ, 674, L109
Sheeley, N. R., Jr., et al. 2008b, ApJ, 675, 853
Smith, C. W., L'Heureux, J., Ness, N. F., Acuña, M. H., Burlaga, L. F., & Scheifele, J. 1998, Space Sci. Rev., 86, 613
Smith, E. J., Balogh, A., Neugebauer, M., & McComas, D. 1995, Geophys. Res. Lett., 22, 3381
St. Cyr, O. C., et al. 2000, J. Geophys. Res., 105, 18169
Steinberg, J. T., Gosling, J. T., Skoug, R. M., & Wiens, R. C. 2005, J. Geophys. Res., 110, A06103
Thernisien, A. F. R., Howard, R. A., & Vourlidas, A. 2006, ApJ, 652, 763
Tsurutani, B. T., Ho, C. M., Arballo, J. K., Smith, E. L., Goldstein, B. E., Neugebauer, M., Balogh, A., & Feldman, W. C. 1996, J. Geophys. Res., 101, 11027
Wang, Y.-M. 2008, Space Sci. Rev., 144, 383
Wood, B. E., Howard, R. A., Plunkett, S. P., & Socker, D. G. 2009, ApJ, 694, 707
Wood, B. E., Howard, R. A., & Socker, D. G. 2010, ApJ, 715, 1524